Exogenous H₂S mitigates myocardial fibrosis in diabetic rats through suppression of the canonical Wnt pathway

RUI YANG[1], QIANG JIA[2], SHAN-FENG MA[2], YA WANG[1], SHOMAILA MEHMOOD[1] and YAN CHEN[1]

[1]School of Life Sciences, Anhui University, Hefei, Anhui 230601;
[2]Department of Physiology, Bengbu Medical College, Bengbu, Anhui 233030, P.R. China

Abstract. Hydrogen sulfide (H₂S) has antifibrotic activity in the kidneys, heart, lungs, and other organs. The present study investigated the protective activity of exogenous H₂S against myocardial fibrosis in a rat model of diabetes. Animals were assigned to normal control, diabetes mellitus (DM), DM + sodium hydrosulfide (NaHS; DM + NaHS) and NaHS groups. Fasting blood glucose (FBG), cardiac function and hydroxyproline were monitored. Heart histomorphology and ultrastructure were additionally evaluated. Wnt1-inducible signaling pathway protein (WISP)-1 protein expression in the myocardium was determined by immunohistochemical staining. Matrix metalloprotease (MMP)-2, tissue inhibitor of metalloproteinase (TIMP)-2, collagens, and canonical Wnt and transforming growth factor (TGF)-β1/SMAD family member 3 (Smad3) pathway-related proteins were assessed by western blotting. Cardiac function was decreased, and myocardial injury, hypertrophy and fibrosis were increased in the diabetes model rats. MMP-2 expression was decreased, and the expressions of WISP-1, TIMP-2, collagens, and canonical Wnt and TGF-β1/Smad3 pathway-related proteins were increased in the myocardia of the diabetes model rats. The present results indicated that the canonical Wnt pathway promoted diabetic myocardial fibrosis by upregulating the TGF-β1/Smad3 pathway. Except for FBG, exogenous H₂S ameliorated the changes in diabetes-associated indices in rats in the DM + NaHS group. The results are consistent with H₂S protection of streptozotocin-induced myocardial fibrosis in the diabetes model rats by downregulation of the canonical Wnt and TGF-β1/Smad3 pathway and decreased myocardial collagen deposition.

Correspondence to: Dr Yan Chen, School of Life Sciences, Anhui University, 111 Jiulong Road, Hefei, Anhui 230601, P.R. China
E-mail: chenyan91030@yahoo.com

Introduction

Diabetic cardiomyopathy (DCM) is a cardiovascular complication of diabetes that contributes to its morbidity and mortality rates. DCM is responsible for heart muscle dysfunction in the absence of primary risks, including hypertension or coronary artery disease (1). Myocardial fibrosis is present in the majority of cardiac pathologies, including DCM (2). Among the variety of cell types present in the heart, cardiac fibroblasts and cardiomyocytes are the most prominent (3). Increased secretion of extracellular matrix (ECM) components and growth factors by cardiac fibroblasts occurs during the onset and progression of myocardial fibrosis (4). In myocardial fibrosis, the proliferation of cardiac fibroblasts and production of ECM components, including collagens, are promoted by activation of the transforming growth factor (TGF)-β1/SMAD family member 3 (Smad3) signaling pathway (5-7).

Wnt proteins act as signaling molecules to accelerate cell proliferation, differentiation and migration (8). Wnt signaling comprises two highly conserved pathways that participate in diverse cellular physiological and pathological processes (9,10). The canonical β-catenin-dependent pathway participates in myocardial fibrosis, and may be a novel therapeutic target in fibrotic diseases (11). In the canonical Wnt pathway, β-catenin is an intracellular transducer of extracellular signals that activate downstream target genes, including Wnt1-inducible signaling pathway protein (WISP)-1 (12). WISP-1 induces fibroblast proliferation, ECM deposition and cardiomyocyte hypertrophy (13). The canonical Wnt and TGF-β/Smad3 pathways are both active in myocardial fibrosis (14,15). Glycogen synthase kinase (GSK)-3β, which is a key component of the canonical Wnt pathway, alleviates myocardial injury in the ischemic myocardium by binding to Smad3 to negatively regulate the TGF-β1 signaling pathway (16).

Hydrogen sulfide (H₂S) is one of three gaseous signaling molecules in mammals, and it protects against injury of the kidneys, heart, lungs, brain and other organs (17,18). Sodium hydrosulfide (NaHS) is frequently utilized as an exogenous H₂S donor (19). It has been reported that H₂S alleviated myocardial fibrosis in spontaneously hypertensive rats by inhibiting the TGF-β1/Smad pathway (20). To the best of the authors' knowledge, evidence that the canonical Wnt pathway is involved in the protective activity of exogenous H₂S in diabetes-associated myocardial fibrosis is lacking. The present

study investigated the activity of exogenous H$_2$S in a rat model of diabetic myocardial fibrosis through negative regulation of the canonical Wnt pathway, and downregulation of WISP-1 and the TGF-β1/Smad3 pathway.

Materials and methods

Animals. A total of 32 male Sprague-Dawley rats of 6-7 weeks of age (weighing 160-200 g) were provided by The Animal Administration Center of Bengbu Medical College. The rats were given a standard laboratory diet and fresh drinking water, and housed in a controlled environment at 50-60% humidity and 21-23°C constant temperature with a 12 h light/dark cycle. All the experimental procedures and protocols of the present study were approved by the Animal Ethics Committee of Anhui University.

Reagents. Streptozotocin, NaHS and BSA (cat. no. B2064) were provided by Sigma-Aldrich; Merck KGaA. Goat serum (cat. no. 16210064) was provided by Thermo Fisher Scientific, Inc. A hydroxyproline (Hyp) assay kit (cat. no. A030-3) was provided by Nanjing Jiancheng Bioengineering Institute. An ECL detection reagent (cat. no. WBKLS0100) was provided by EMD Millipore. A bicinchoninic acid (BCA) protein assay kit, cell lysis buffer (cat. no. P0013) and phenylmethanesulfonyl fluoride (PMSF; cat. no. ST506) were provided by Beyotime Institute of Biotechnology. Rabbit anti-β-catenin (cat. no. 51067-2-AP; 1:500), anti-total GSK-3β (cat. no. 22104-1-AP; 1:500), anti-collagen-I (cat. no. 14695-1-AP; 1:500) and anti-collagen-III (cat. no. 22734-1-AP; 1:500) antibodies were provided by Wuhan Sanying Biotechnology. Rabbit anti-phosphorylated (p)-GSK-3β (Ser 9; cat. no. 9323; 1:1,000), anti-Smad3 (cat. no. 9513; 1:1,000) and anti-p-Smad3 (cat. no. 9520; 1:1,000) antibodies were from Cell Signaling Technology, Inc. Rabbit anti-TGF-β1 (cat. no. ab92486; 1:1,000) and anti-GAPDH (cat. no. ab181602; 1:2,000) antibodies were provided by Abcam. Rabbit anti-matrix metalloprotease-2 (MMP-2; cat. no. A00286; 1:500), anti-tissue inhibitor of metalloproteinase-2 (TIMP-2; cat. no. BA0576; 1:500) and anti-WISP-1 (cat. no. BA3035) antibodies, and horseradish peroxidase-conjugated goat anti-rabbit secondary antibody (cat. no. BA1054) were provided by Wuhan Boster Biological Technology, Ltd.

Experimental grouping and treatment. Rats were allocated into four groups at random: Normal control (NC) group, diabetes mellitus (DM) group, DM + NaHS group and NaHS group (n=8/group). A single intraperitoneal (i.p.) injection of streptozotocin at a dose of 55 mg/kg, dissolved in 0.1 mol/l citrate buffer at a pH of 4.5, was administered to 12 h-fasted rat to induce Type 1 DM. An i.p. injection of equal amount of citrate buffer was administered to the rats in the NC group. After streptozotocin-injection for 72 h, 12 h-fasted rats with tail vein blood glucose concentrations >16.7 mmol/l were grouped as diabetic rats. Following successful establishment of the diabetic model, NaHS (56 μmol/kg/day; i.p.) was administered in the DM + NaHS and NaHS groups until the end of the 8th week, according to a previously described method (21,22). Rats in the NC and DM groups received daily injected doses of the equal volume of saline solution, using the same dosing protocol.

Ventricular hemodynamic measurements. The cardiac function was assessed according to a previous study (21). Rats were weighed and anesthetized with chloral hydrate (400 mg/kg; i.p.), and then a cannula was incubated into the trachea. The right carotid artery of each rat was detached and canulated into the left ventricle. Following stabilization for 10 min, the Med-Lab Biological Recording system (Medease Science and Technology Co., Ltd.) was utilized to measure left ventricular end-diastolic pressure (LVEDP), maximal rise rate of left ventricular pressure (+dp/dt_{max}), maximal fall rate of left ventricular pressure (-dp/dt_{max}) and left ventricular systolic pressure (LVSP).

Measurement of blood glucose, heart weight/body weight (HW/BW) and myocardial Hyp content. Following ventricular hemodynamic measurement, the blood from the tail vein was obtained to measure the fasting blood glucose (FBG) level using a portable glucometer (Accu-Chek; Roche). In order to calculate the HW/BW ratio, the rats were sacrificed following 8 weeks of treatment. Their hearts were removed, washed in chilled saline solution, dried and then weighed. The myocardium of each rat was homogenized and treated in 1 ml 6 mol/l HCl at 100°C, for 6 h. Following pH adjustment to a range of 6.0-6.8, 25 mg activated carbon was mixed in 4 ml diluted hydrolyzation products. All the samples were centrifuged at 1,123 x g for 10 min at 4°C and the supernatant fluids were collected to calculate the Hyp concentration using the Hyp assay kit.

Histomorphological evaluation. The myocardium of each rat was fixed using 10% formalin solution for 1 day at room temperature, embedded in paraffin at room temperature, and then sectioned into 5 μm-thick slices. After the tissue slides were treated using dimethylbenzene twice for 10 min at room temperature, a series of ethanol solutions (100, 95, 90, 80 and 70%) were used to rehydrate them for 5 min at each concentration. Then, the slides were dyed using Harris hematoxylin and 0.5% eosin (H&E) at room temperature, for 5 min and 2 min, respectively. Other tissue slides were dyed with Masson's trichrome reagent, as previously described (23). Sections were observed with a light microscope (magnification x400) and images were captured for morphological study. Image-Pro Plus 6.0 software (Media Cybernetics, Inc.) was utilized to calculate the collagen volume fraction (CVF) in myocardium. A total of five sections of each sample were selected at random and their average was calculated for further analysis.

Ultrastructure analysis. Tissue ultrathin sections at a thickness of 70 nm were prepared, as previously described (23). The heart was cut into 1x1x1 mm cubes and fixed with 2.5% glutaraldehyde for 5 h at 4°C, and post-fixed in 1% osmium tetroxide for 1 h at room temperature. Myocardial tissue was embedded in Epon812 for 2 h at room temperature and then cut into ultrathin sections. Uranyl acetate and lead citrate were used to stain the ultrathin sections at room temperature, for 30 and 15 min respectively, and then observed using a JEOL JEM-1230 transmission electron microscope (JEOL, Ltd.).
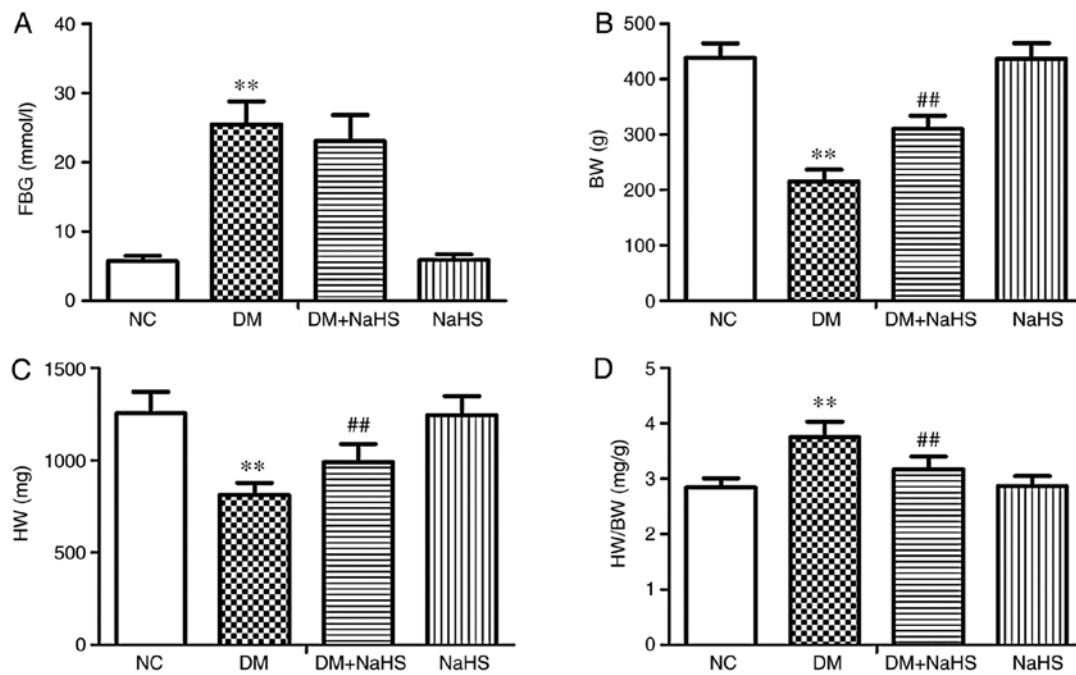
Figure 1. Effects of exogenous hydrogen sulfide on FBG and HW/BW. (A) FBG, (B) BW, (C) HW and (D) HW/BW in the different groups. Data are presented as the mean ± SD. n=8/group. [**]P<0.01 vs. NC group; [##]P<0.01 vs. DM group. FBG, fasting blood glucose; BW, body weight; HW, heart weight; HW/BW, heart weight/body weight; NC, normal control; DM, diabetes mellitus; NaHS, sodium hydrosulfide.

Immunohistochemical analysis. Myocardial WISP-1 protein expression was detected by immunohistochemistry. Immunohistochemical staining was performed using an immunohistochemical detection kit (cat. no. PV6001; Beijing Zhongshan Jinqiao Biotechnology Co., Ltd.). The paraffin-fixed myocardium was cut into 4 μm-thick slides, treated with dimethylbenzene twice for 10 min at room temperature and graded alcohol (100, 95, 90, 80 and 70%) for 5 min at each concentration at room temperature, and rinsed in PBS at room temperature. After blocking endogenous peroxidase activity with H_2O_2 (3%) at room temperature for 10 min, the slides were rinsed with PBS and boiled at 95°C for antigen retrieval in citrate buffer at a pH of 6.0 for 15 min. The slides were rinsed with PBS, blocked with goat serum (10%) at room temperature for 30 min, and then incubated at 4°C overnight with rabbit anti-WISP-1 polyclonal antibody (1:50). After washing with PBS, the tissue sections were treated with goat anti-rabbit immunoglobulin G secondary antibody (1:500) for 1 h at 37°C. After washing with PBS, tissue slides were stained with diaminobenzidine for 5 min at room temperature. The slides were dyed using hematoxylin for 1 min at room temperature, dehydrated and mounted. Histological sections were observed by light microscopy (magnification x400) and imaged. A total of five sections of each sample were selected at random and analyzed using Image-Pro Plus 6.0 software.

Western blotting assay. The myocardium of each rat was lysed with a mixed protein extraction buffer containing lysis buffer (990 μl) and PMSF (10 μl). The protein quantification was performed using a BCA assay kit. An equal amount of protein (40 μg) was isolated by SDS-PAGE on 10% gels, and then transferred to PVDF membranes. Membranes to be incubated with p-GSK-3β and p-Smad3 antibodies, were blocked with 5% BSA in Tris-buffered saline Tween-20 (TBST) at 37°C for 2 h, and the membranes to be incubated with MMP-2, TIMP-2, β-catenin, collagen-I, collagen-III, Smad3, GSK-3β, TGF-β1 and GAPDH antibodies were blocked with 5% non-fat milk in TBST at 37°C for 2 h. Afterwards, membranes were incubated at 4°C overnight with the mentioned primary antibodies. A horseradish peroxidase-conjugated goat anti-rabbit secondary antibody was used at a 1:5,000 dilution for 1 h at room temperature. The visualization of protein bands was detected using ECL reagent and scanned using the ChemiDoc XRS system (Bio-Rad Laboratories, Inc.). The band density was determined using Quantity One Version 4.6.6 software (Bio-Rad Laboratories, Inc.).

Statistical analysis. All the experimental data are presented as the mean ± SD. All tests were repeated three times. The statistical analysis of the results was conducted using SPSS version 17.0 software (SPSS, Inc.). The comparisons among groups were examined using ANOVA and Newman-Keuls test. P<0.05 was considered to indicate a statistically significant difference.

Results

Effects of exogenous H_2S on FBG and HW/BW. Exogenous H_2S alleviated myocardial hypertrophy in diabetes model rats, with increased BW and HW, and a decreased HW/BW ratio compared with the DM group. As shown in Fig. 1, FBG and HW/BW were significantly elevated, and BW and HW were significantly reduced in DM model rats compared with NC rats, which indicated that diabetes induced myocardial hypertrophy. Compared with the DM group, exogenous H_2S significantly decreased the HW/BW ratio but not FBG, and
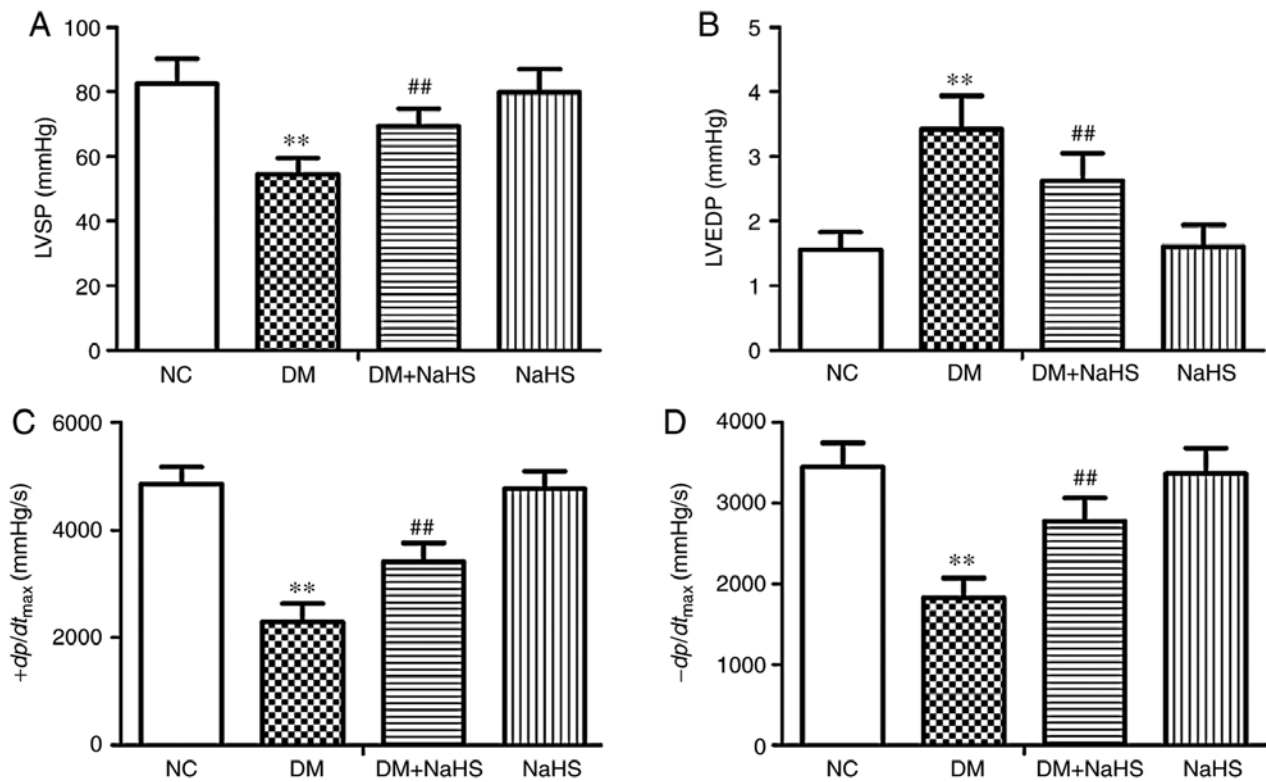
Figure 2. Effect of exogenous hydrogen sulfide on cardiac function in the different groups. (A) LVSP, (B) LVEDP, (C) $+dp/dt_{max}$, (D) $-dp/dt_{max}$ in the different groups. Data are presented as the mean ± SD. n=8/group. **P<0.01 vs. NC group; $^{\#\#}$P<0.01 vs. DM group. LVSP, left ventricular systolic pressure; LVEDP, left ventricular end diastolic pressure; $+dp/dt_{max}$, maximal rise rate of left ventricular pressure; $-dp/dt_{max}$, maximal fall rate of left ventricular pressure; NC, normal control; DM, diabetes mellitus; NaHS, sodium hydrosulfide.

significantly increased BW and HW in the DM + NaHS group. There were no statistically significant differences in FBG, HW/BW, BW and HW between the NC and NaHS groups.

Effects of exogenous H$_2$S on ventricular hemodynamics. Exogenous H$_2$S ameliorated diabetic cardiac dysfunction by decreasing LVEDP, and increasing LVSP and $\pm dp/dt_{max}$, compared with the DM group. As shown in Fig. 2, LVSP, $+dp/dt_{max}$ and $-dp/dt_{max}$ were significantly decreased and LVEDP was significantly increased in the DM model rats compared with the NC rats. Exogenous H$_2$S treatment significantly decreased LVEDP, and increased LVSP, $+dp/dt_{max}$ and $-dp/dt_{max}$ in the DM + NaHS rats compared with the DM rats.

Effects of exogenous H$_2$S on myocardial histology and ultrastructure. Myocardial fibers were neatly organized and the cell nuclei were clearly defined in H&E stained tissue from normal rats. The arrangement of cardiomyocytes in the myocardium of DM rats was disordered and the majority of myocardial fibers were broken. Exogenous H$_2$S markedly reduced the severity of histological damage in the DM + NaHS group (Fig. 3A).

The ultrastructure of myocardial cells in NC rats included cardiac sarcomeres of uniform length and organization, and mitochondria with a normal appearance. In the DM rats, the cardiomyocyte ultrastructure was severely disturbed and the mitochondria were swollen. Exogenous H$_2$S decreased the injury of the myocardial ultrastructure in the DM + NaHS group. There were no obvious pathological changes in the NaHS group compared with the control group (Fig. 3B).

Exogenous H$_2$S reduced the severity of histomorphological and ultrastructural injury in DCM.

Effects of exogenous H$_2$S on myocardial collagen deposition. Masson's trichrome stained heart tissue from control rats exhibited small amounts of interstitial collagen fibers and cardiomyocytes with a normal, uniform arrangement. In the DM model rats, large amounts of interstitial and perivascular collagen fibers were present in the myocardial tissue. Exogenous H$_2$S treatment reduced the extent of collagen fiber deposition in diabetic myocardia. There were no obvious histological differences in the NC and NaHS groups (Fig. 4A). Quantitative analysis (Fig. 4B and C) revealed that the CVF and Hyp contents were significantly elevated in the diabetic model rats compared with the normal controls. Compared with the DM group, exogenous H$_2$S significantly reduced the CVF and Hyp levels in DM + NaHS rats. The results suggested that exogenous H$_2$S alleviated diabetic myocardial fibrosis by decreasing collagen deposition and Hyp content.

Effects of exogenous H$_2$S on myocardial ECM proteins. As shown in Fig. 5A, myocardial MMP-2 protein expression was reduced, and the expression of collagen-I, collagen-III and TIMP-2 were increased in the diabetes model rats compared with the normal controls. In the DM + NaHS group, exogenous H$_2$S increased myocardial MMP-2 expression, and reduced the expression of TIMP-2 and collagen proteins compared with the DM group. The results suggested that exogenous H$_2$S
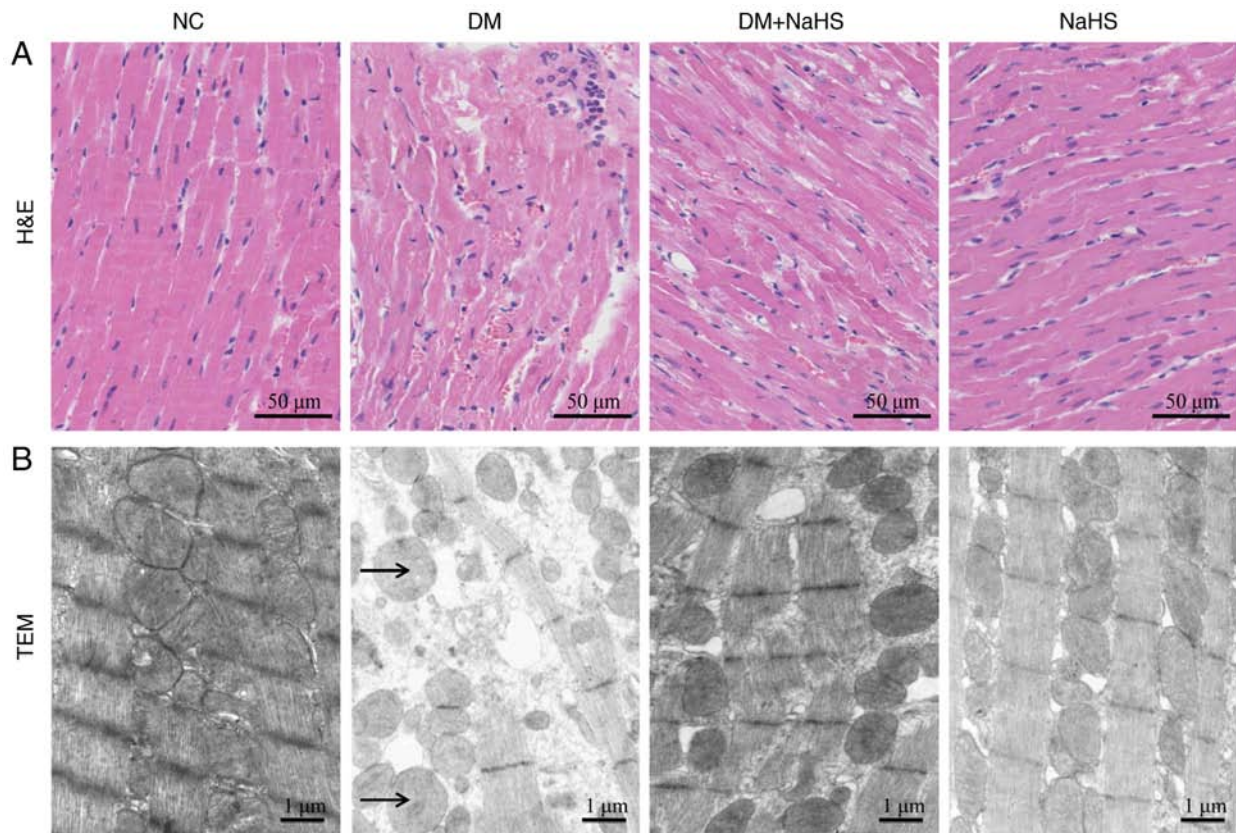
Figure 3. Effects of exogenous hydrogen sulfide on histological and ultrastructural alterations in myocardial tissues. (A) Representative H&E staining of myocardial tissues. (B) Representative transmission electron micrographs of myocardial tissues. Arrows indicate the swollen mitochondria. H&E, hematoxylin and eosin; NC, normal control; DM, diabetes mellitus; NaHS, sodium hydrosulfide; TEM, transmission electron microscope.

downregulated collagen expression by regulating MMP/TIMP activity.

Effects of exogenous H_2S on the myocardial TGF-β1/Smad3 pathway. As shown in Fig. 5B, the expression of TGF-β1, Smad3, p-Smad3 and p-Smad3/Smad3 were increased in the diabetes model rats compared with the NC group, demonstrating that the TGF-β1/Smad3 pathway was active in diabetic myocardial fibrosis in the animal model. Exogenous H_2S decreased the expression of TGF-β1/Smad3 pathway-related proteins in the DM + NaHS group compared with the DM group. The results suggested that exogenous H_2S downregulated the TGF-β1/Smad3 pathway in DCM.

Effects of exogenous H_2S on the canonical Wnt pathway and WISP-1 expression in myocardial tissue. Myocardial GSK-3β expression was reduced, and p-GSK-3β, β-catenin and p-GSK-3β/GSK-3β expression were increased in the diabetes model rats compared with the NC group. The results suggested that canonical Wnt signaling was involved in diabetic myocardial fibrosis. Exogenous H_2S significantly inhibited the changes in expression of Wnt-signaling proteins in the DM + NaHS group compared with the DM group (Fig. 6A). The results of WISP-1 immunohistochemical staining in cardiomyocytes are shown in Fig. 6B and C. WISP-1 expression was significantly higher in the diabetes model rats compared with the NC group. Exogenous H_2S decreased the WISP-1 expression in the DM + NaHS group compared with the DM group.

There were no significant differences in WISP-1 expression between the NC and NaHS groups. The results suggested that exogenous H_2S downregulated the canonical Wnt pathway and WISP-1 expression in diabetic myocardial tissues.

Discussion

Hyperglycemia causes changes in cardiac contractility and structure that result in diastolic and systolic dysfunction, and interstitial and perivascular myocardial fibrosis, characteristic of DCM (24). In a previous study, cardiac hypertrophy, fibrosis and dysfunction all occurred in diabetes model rats (25). Extensive deposition of ECM, including collagen-I and collagen-III, associated with diabetes results in increased stiffness of the heart that affects cardiac function (26). In the present study, the rat model of diabetes demonstrated that cardiac function, BW and HW were decreased, and FBG, HW/BW, CVF and Hyp were increased compared with NC rats. The histomorphological analysis showed that diabetes induced cardiomyocyte injury and increased deposition of collagen fibers in the heart.

H_2S is an endogenous gas signaling molecule, which plays an important role in many physiological processes in mammalian systems, including the nervous, cardiovascular and urinary systems (27). H_2S plays a protective role in anti-oxidative, anti-inflammatory and anti-apoptosis activities in diabetic rats (21,22,28). The present study identified that, in contrast to diabetic rats, exogenous H_2S increased the weights
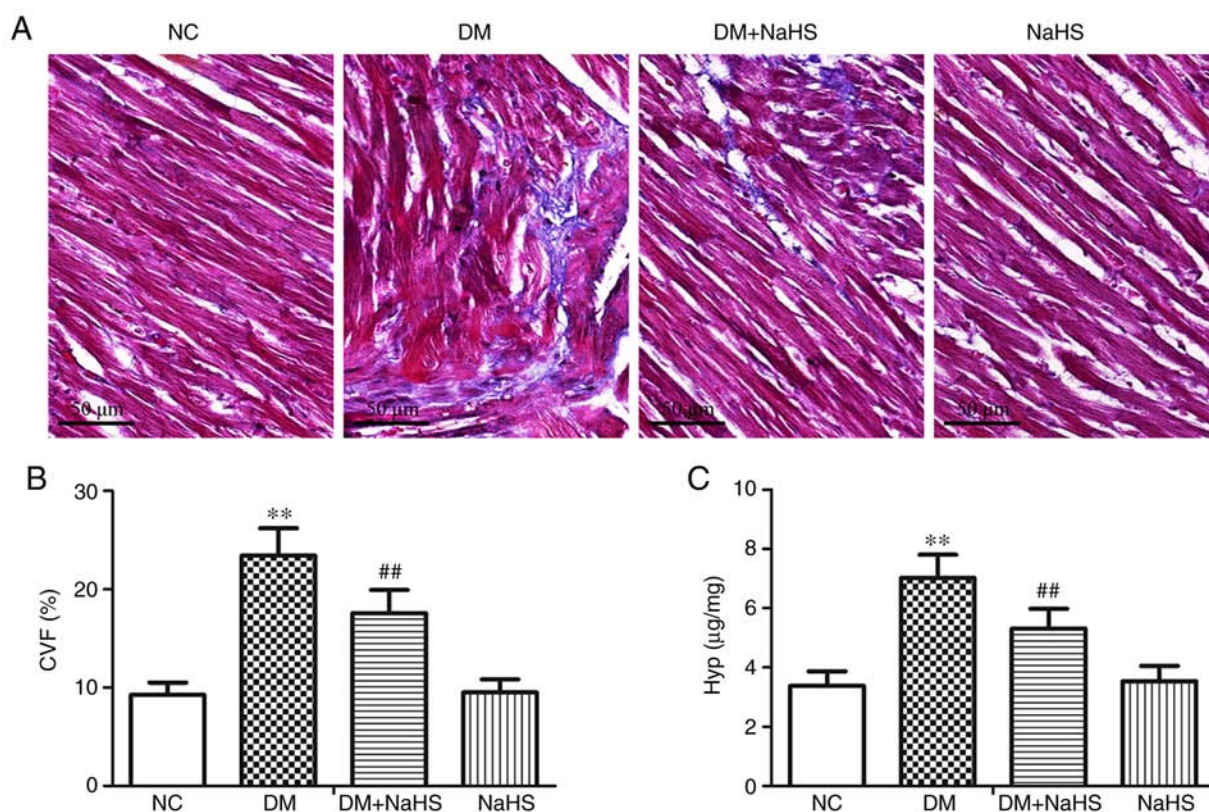
Figure 4. Effect of exogenous hydrogen sulfide on collagen deposition in myocardial tissues. (A) Representative Masson's trichrome staining of myocardial tissues. Levels of (B) CVF and (C) Hyp content in the different groups. Data are presented as the mean ± SD. n=8/group. **P<0.01 vs. NC group; $^{##}$P<0.01 vs. DM group. CVF, collagen volume fraction; Hyp, hydroxyproline; NC, normal control; DM, diabetes mellitus; NaHS, sodium hydrosulfide.
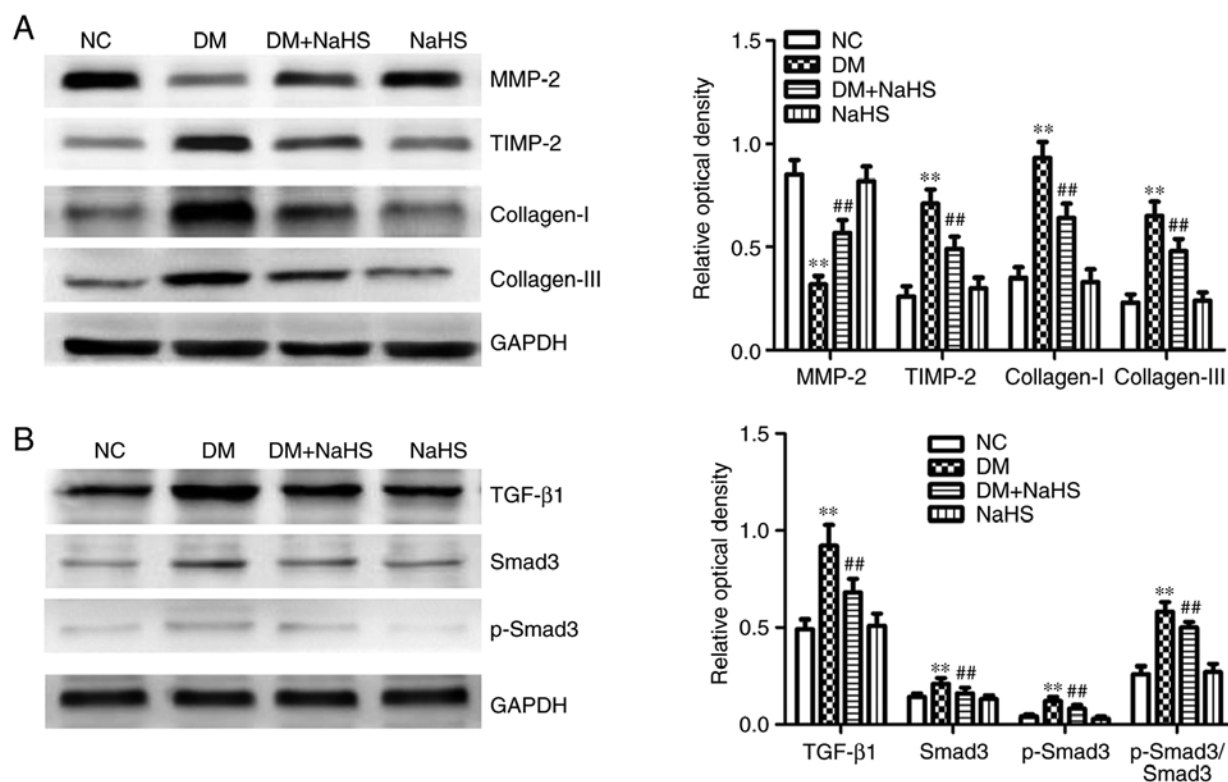

Figure 5. Effect of exogenous hydrogen sulfide on extracellular matrix-associated proteins and the TGF-β1/Smad3 pathway in myocardial tissues. (A) Protein expression levels of MMP-2, TIMP-2, collagen-I and collagen-III in myocardium. (B) Expression levels of TGF-β1/Smad3 pathway-related proteins in myocardium. Data are presented as the mean ± SD. n=8/group. **P<0.01 vs. NC group; $^{##}$P<0.01 vs. DM group. TGF-β1, transforming growth factor-β1; Smad3, SMAD family member 3; MMP-2, matrix metalloproteinase-2; TIMP-2, tissue inhibitor of metalloproteinase-2; NC, normal control; DM, diabetes mellitus; NaHS, sodium hydrosulfide; p-, phosphorylated.
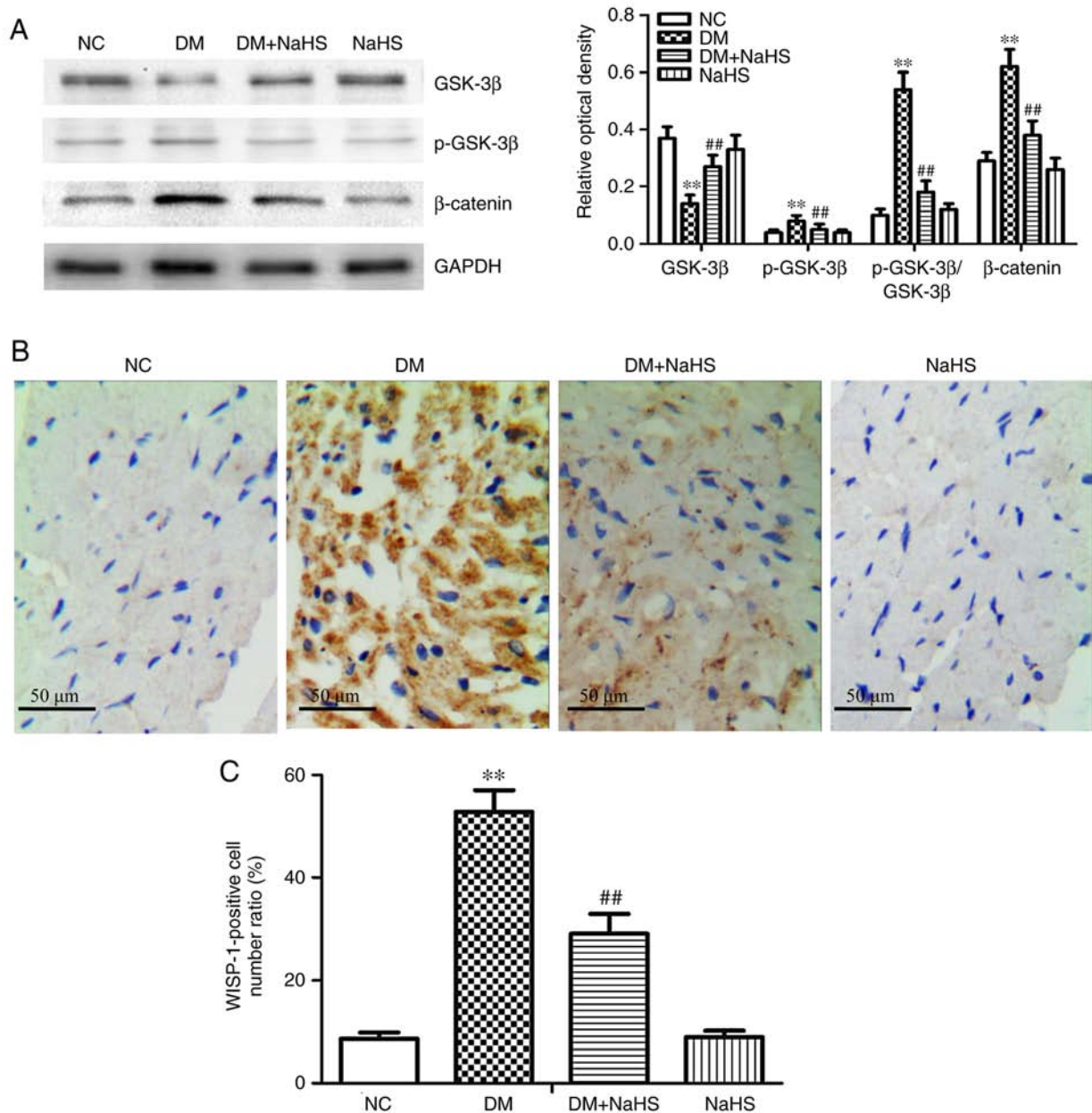
Figure 6. Effect of exogenous hydrogen sulfide on the canonical Wnt pathway and WISP-1 expression in myocardial tissues. (A) Western blot analysis of the protein expression of β-catenin, GSK-3β and p-GSK-3β. (B) Immunohistochemical study of WISP-1 was performed in myocardial tissues. (C) Ratio of WISP-1-positive cells in each group. Data are presented as the mean ± SD. n=8/group. **$P<0.01$ vs. NC group; ##$P<0.01$ vs. DM group. WISP-1, Wnt1-inducible signaling pathway protein-1; GSK-3β, glycogen synthase kinase-3β; p-, phosphorylated; NC, normal control; DM, diabetes mellitus; NaHS, sodium hydrosulfide.

of the body and heart, and decreased the histomorphological damages in the DM + NaHS group, which further suggested that exogenous H₂S serves a protective role in diabetic rats.

It was previously reported that H₂S could regulate cardiac function in mammals (29). The effects of H₂S have been described in models of cardiac injury, such as myocardial ischemia/reperfusion injury (30), and spontaneously hypertensive-, isoproterenol-, and diabetes-induced myocardial injury (20,31,32). H₂S has previously been found to protect against myocardial injury and fibrosis in diabetic rats (33), but the cellular mechanisms were not well investigated. The present study did not identify any harmful effects of exogenous H₂S in normal rats; however, it protected diabetes model rats by reducing cardiac hypertrophy, dysfunction and fibrosis. The

present results provide insight for the current understanding of the mechanism of the antifibrotic effects of H₂S on diabetic hearts.

Canonical Wnt signaling promotes fibroblast activation and proliferation (34). Under normal conditions, the canonical Wnt pathway is not active. In the absence of Wnt, β-catenin is degraded by the axin/adenomatous polyposis coli/GSK3β complex, which results in a low level of cytosolic β-catenin (35). Under conditions of stress, the Wnt protein binds to its cell surface receptor, which activates disheveled proteins, leading to the dissociation of GSK-3β from the complex (36). β-catenin is not degraded, and accumulates in the cytoplasm and translocates into the nucleus, where it binds to T-cell factor/lymphoid enhancer factor and then activates WISP-1 (37). GSK-3β is
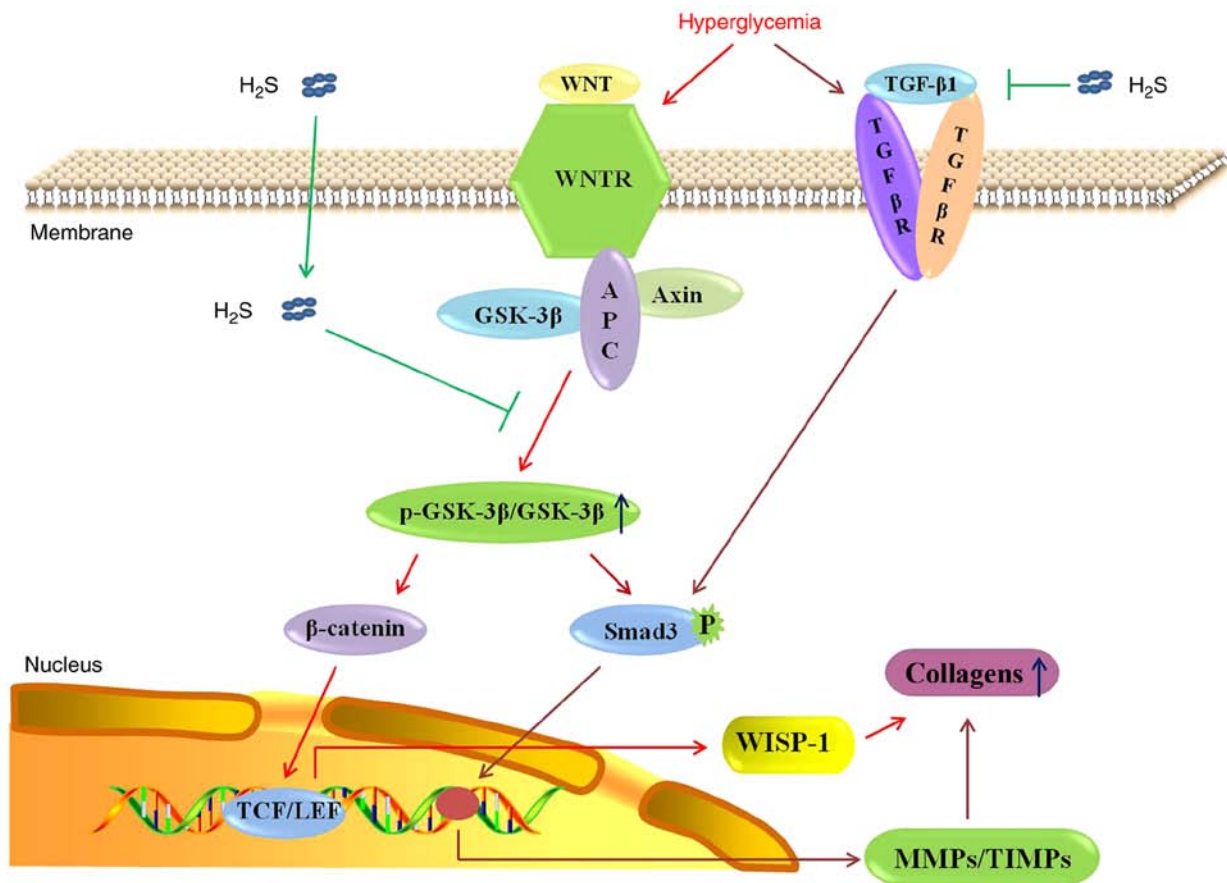
Figure 7. Possible antifibrotic mechanism of exogenous hydrogen sulfide in diabetic cardiomyocytes. H₂S, hydrogen sulfide; TGF-β1, transforming growth factor-β1; R, receptor; GSK-3β, glycogen synthase kinase-3β; APC, adenomatous polyposis coli; p-, phosphorylated; Smad3, SMAD family member 3; P, phosphate; TCF/LEF, T-cell factor/lymphoid enhancer factor; WISP-1, Wnt1-inducible signaling pathway protein-1; MMP, matrix metalloproteinase; TIMP, tissue inhibitor of metalloproteinase.

a highly conserved serine/threonine kinase present in the canonical Wnt pathway. Its activity is inhibited by phosphorylation of the Ser9 site (38). Inhibition of GSK-3β has been shown to induce dermal fibrosis by activating the canonical Wnt pathway (39). The present study found that, in contrast to normal rats, diabetes increased β-catenin, p-GSK-3β, WISP-1 and p-GSK-3β/GSK-3β expression, and decreased the expression of the GSK-3β protein. The results are consistent with the participation of the canonical Wnt pathway in diabetes-induced myocardial injury and fibrosis in this rat model. H₂S-releasing aspirin has been reported to strongly inhibit the growth of Jurkat T-leukemia cells and the expression of β-catenin (40). H₂S has also been reported to preserve synaptic plasticity, protecting against vascular dementia-induced damage, at least in part by increasing GSK-3β expression (41). In the present study, exogenous H₂S significantly decreased the expression of canonical Wnt pathway proteins in H₂S-treated diabetes model rats, indicating that the antifibrotic activity of H₂S in the diabetic myocardium may be directly related to negative regulation of the canonical Wnt pathway.

The TGF-β1/Smad3 pathway is active in lung, renal and liver fibrosis; it activates fibrosis mediators, and suppresses the degradation of the ECM by regulating MMP/TIMP activity (42-44). MMPs are endogenous zinc-dependent enzymes, and it is known that downregulation of MMP-2 occurs at the onset of myocardial fibrosis in DCM (45,46).

MMP-2 degrades collagen by digesting fibrillar collagen peptides and newly formed collagen fibers (47). MMP activity is controlled by TIMPs (48). Li *et al* (49) reported that the activity of TIMP-2 is increased in myocardial fibrosis associated with diabetes. In the present study, MMP-2 was decreased in diabetes model rats, and the expression of TIMP-2 and TGF-β1/Smad3 pathway proteins was increased, implicating the involvement of the TGF-β1/Smad3 pathway in diabetic myocardial fibrosis. Exogenous H₂S significantly reduced the changes in the diabetes-associated proteins in the NaHS-treated diabetes model rats. The results are suggested that the antifibrotic activity of H₂S was mediated by downregulation of the TGF-β1/Smad3 pathway and maintenance of MMP/TIMP activity.

A previous study identified correlations of activities of the canonical Wnt and TGF-β1/Smad3 pathways in myocardial fibrogenesis (15). Decreased β-catenin can inhibit TGF-β1-induced myofibroblast transformation (50), and a decrease in the activity or expression of GSK-3β resulted in increased activity and stability of Smad3 protein (51). In the present study, GSK-3β expression was decreased, and p-GSK-3β, Smad3, β-catenin and TGF-β1 expression were increased in diabetes model rats. The present results are consistent with upregulation of the expression of TGF-β1/Smad3 pathway proteins in the diabetic myocardium through the canonical Wnt pathway. Exogenous H₂S

inhibited the changes in the expression of pathway-related proteins observed in the myocardia of the diabetes model rats. The aim of the present study was to demonstrate that exogenous H_2S negatively regulated the canonical Wnt pathway and downregulated the TGF-β1/Smad3 pathway in the diabetic myocardium. Further studies are required to detect the associations of activities of the canonical Wnt and TGF-β1/Smad3 pathways, and to further confirm the mechanism of action of H_2S in the antifibrotic signaling pathways. In conclusion, H_2S attenuated streptozotocin-induced diabetic myocardial fibrosis in rats. The molecular mechanism may involve negative regulation of the canonical Wnt pathway, downregulation of WISP-1 and the TGF-β1/Smad3 pathway, and decreased collagen deposition, as shown in Fig. 7. The canonical Wnt pathway may be a novel target for exogenous H_2S as a treatment of DCM.

Acknowledgements

Funding

Availability of data and materials

The data generated or analyzed during this study are included in this published article.

Authors' contributions

RY, QJ, SFM and YC made substantial contributions to the conception and design of the experiments. RY, QJ, YW and SM conducted the experiments. RY and QJ analyzed the experimental data and wrote the manuscript. YC and SM edited and revised the manuscript. All authors read and approved the final manuscript.

Ethics approval and consent to participate

All experimental protocols were approved by the Animal Ethics Committee of Anhui University.

Patient consent for publication

Not applicable.

Competing interests

The authors declare that they have no competing interests.

References

1. Gilca GE, Stefanescu G, Badulescu O, Tanase DM, Bararu I and Ciocoiu M: Diabetic cardiomyopathy: Current approach and potential diagnostic and therapeutic targets. J Diabetes Res 2017: 1310265, 2017.

2. Zou C, Liu X, Xie R, Bao Y, Jin Q, Jia X, Li L and Liu R: Deferiprone attenuates inflammation and myocardial fibrosis in diabetic cardiomyopathy rats. Biochem Biophys Res Commun 486: 930-936, 2017.

3. Moore-Morris T, Guimarães-Camboa N, Yutzey KE, Pucéat M and Evans SM: Cardiac fibroblasts: From development to heart failure. J Mol Med (Berl) 93: 823-830, 2015.

4. Deb A and Ubil E: Cardiac fibroblast in development and wound healing. J Mol Cell Cardiol 70: 47-55, 2014.

5. Su SA, Yang D, Wu Y, Xie Y, Zhu W, Cai Z, Shen J, Fu Z, Wang Y, Jia L, et al: EphrinB2 regulates cardiac fibrosis through modulating the interaction of Stat3 and TGF-β/Smad3 signaling. Circ Res 121: 617-627, 2017.

6. Han A, Lu Y, Zheng Q, Zhang J, Zhao Y, Zhao M and Cui X: Qiliqiangxin attenuates cardiac remodeling via inhibition of TGF-β1/Smad3 and NF-κB signaling pathways in a rat model of myocardial infarction. Cell Physiol Biochem 45: 1797-1806, 2018.

7. Li X, Han D, Tian Z, Gao B, Fan M, Li C, Li X, Wang Y, Ma S and Cao F: Activation of cannabinoid receptor type II by AM1241 ameliorates myocardial fibrosis via Nrf2-mediated inhibition of TGF-β1/Smad3 pathway in myocardial infarction mice. Cell Physiol Biochem 39: 1521-1536, 2016.

8. Wang Y, Li YP, Paulson C, Shao JZ, Zhang X, Wu M and Chen W: Wnt and the wnt signaling pathway in bone development and disease. Front Biosci (Landmark Ed) 19: 379-407, 2014.

9. Kim W, Kim M and Jho EH: Wnt/β-catenin signalling: From plasma membrane to nucleus. Biochem J 450: 9-21, 2013.

10. Angers S and Moon RT: Proximal events in wnt signal transduction. Nat Rev Mol Cell Biol 10: 468-477, 2009.

11. Tao H, Yang JJ, Shi KH and Li J: Wnt signaling pathway in cardiac fibrosis: New insights and directions. Metabolism 65: 30-40, 2016.

12. Xu L, Corcoran RB, Welsh JW, Pennica D and Levine AJ: WISP-1 is a wnt-1- and beta-catenin-responsive oncogene. Genes Dev 14: 585-595, 2000.

13. Colston JT, de la Rosa SD, Koehler M, Gonzales K, Mestril R, Freeman GL, Bailey SR and Chandrasekar B: Wnt-induced secreted protein-1 is a prohypertrophic and profibrotic growth factor. Am J Physiol Heart Circ Physiol 293: H1839-H1846, 2007.

14. Działo E, Tkacz K and Błyszczuk P: Crosstalk between the TGF-β and WNT signalling pathways during cardiac fibrogenesis. Acta Biochim Pol 65: 341-349, 2018.

15. Blyszczuk P, Müller-Edenborn B, Valenta T, Osto E, Stellato M, Behnke S, Glatz K, Basler K, Lüscher TF, Distler O, et al: Transforming growth factor-β-dependent wnt secretion controls myofibroblast formation and myocardial fibrosis progression in experimental autoimmune myocarditis. Eur Heart J 38: 1413-1425, 2017.

16. Lal H, Ahmad F, Zhou J, Yu JE, Vagnozzi RJ, Guo Y, Yu D, Tsai EJ, Woodgett J, Gao E and Force T: Cardiac fibroblast glycogen synthase kinase-3β regulates ventricular remodeling and dysfunction in ischemic heart. Circulation 130: 419-430, 2014.

17. Beltowski J: Hydrogen sulfide in pharmacology and medicine-an update. Pharmacol Rep 67: 647-658, 2015.

18. Salloum FN: Hydrogen sulfide and cardioprotection-mechanistic insights and clinical translatability. Pharmacol Ther 152: 11-17, 2015.

19. Su YW, Liang C, Jin HF, Tang XY, Han W, Chai LJ, Zhang CY, Geng B, Tang CS and Du JB: Hydrogen sulfide regulates cardiac function and structure in adriamycin-induced cardiomyopathy. Circ J 73: 741-749, 2009.

20. Sun L, Jin H, Chen S, Sun L, Huang Y, Liu J, Li Z, Zhao M, Sun Y, Tang C, et al: Hydrogen sulfide alleviates myocardial collagen remodeling in association with inhibition of TGF-β/Smad signaling pathway in spontaneously hypertensive rats. Mol Med 20: 503-515, 2015.

21. Yang R, Jia Q, Liu XF, Wang YY and Ma SF: Effects of hydrogen sulfide on inducible nitric oxide synthase activity and expression of cardiomyocytes in diabetic rats. Mol Med Rep 16: 5277-5284, 2017.

22. Jia Q, Yang R, Liu XF, Wang QY, Lu HY and Ma SF: Sodium hydrosulfide attenuates myocardial injury through activating thioredoxin system in diabetic rats. Xi Bao Yu Fen Zi Mian Yi Xue Za Zhi 33: 1385-1391, 2017 (In Chinese).

23. Jia Q, Yang R, Liu XF, Ma SF and Wang L: Genistein attenuates renal fibrosis in streptozotocin-induced diabetic rats. Mol Med Rep 19: 423-431, 2019.

24. Ward ML and Crossman DJ: Mechanisms underlying the impaired contractility of diabetic cardiomyopathy. World J Cardiol 6: 577-584, 2014.
25. Miki T, Yuda S, Kouzu H and Miura T: Diabetic cardiomyopathy: Pathophysiology and clinical features. Heart Fail Rev 18: 149-166, 2013.
26. Yang R, Jia Q, Liu XF and Ma SF: Effect of genistein on myocardial fibrosis in diabetic rats and its mechanism. Mol Med Rep 17: 2929-2936, 2018.
27. Powell CR, Dillon KM and Matson JB: A review of hydrogen sulfide (H2S) donors: Chemistry and potential therapeutic applications. Biochem Pharmacol 149: 110-123, 2018.
28. Qian LL, Liu XY, Chai Q and Wang RX: Hydrogen sulfide in diabetic complications: Focus on molecular mechanisms. Endocr Metab Immune Disord Drug Targets 18: 470-476, 2018.
29. Calvert JW, Coetzee WA and Lefer DJ: Novel insights into hydrogen sulfide-mediated cytoprotection. Antioxid Redox Signal 12: 1203-1217, 2010.
30. Citi V, Piragine E, Testai L, Breschi MC, Calderone V and Martelli A: The role of hydrogen sulfide and H2S-donors in myocardial protection against ischemia/reperfusion injury. Curr Med Chem 25: 4380-4401, 2018.
31. Liu YH, Lu M, Xie ZZ, Hua F, Xie L, Gao JH, Koh YH and Bian JS: Hydrogen sulfide prevents heart failure development via inhibition of renin release from mast cells in isoproterenol-treated rats. Antioxid Redox Signal 20: 759-769, 2014.
32. Zhou X, An G and Lu X: Hydrogen sulfide attenuates the development of diabetic cardiomyopathy. Clin Sci (Lond) 128: 325-335, 2015.
33. Liu M, Li Y, Liang B, Li Z, Jiang Z, Chu C and Yang J: Hydrogen sulfide attenuates myocardial fibrosis in diabetic rats through the JAK/STAT signaling pathway. Int J Mol Med 41: 1867-1876, 2018.
34. Pistocchi A, Fazio G, Cereda A, Ferrari L, Bettini LR, Messina G, Cotelli F, Biondi A, Selicorni A and Massa V: Cornelia de lange syndrome: NIPBL haploinsufficiency downregulates canonical Wnt pathway in zebrafish embryos and patients fibroblasts. Cell Death Dis 4: e866, 2013.
35. Demunter A, Libbrecht L, Degreef H, De Wolf-Peeters C and van den Oord JJ: Loss of membranous expression of beta-catenin is associated with tumor progression in cutaneous melanoma and rarely caused by exon 3 mutations. Mod Pathol 15: 454-461, 2002.
36. Shi J, Li F, Luo M, Wei J and Liu X: Distinct roles of Wnt/β-catenin signaling in the pathogenesis of chronic obstructive pulmonary disease and idiopathic pulmonary fibrosis. Mediators Inflamm 2017: 3520581, 2017.
37. Zhao X, Hua Y, Chen H, Yang H, Zhang T, Huang G, Fan H, Tan Z, Huang X, Liu B and Zhou Y: Aldehyde dehydrogenase-2 protects against myocardial infarction-related cardiac fibrosis through modulation of the Wnt/β-catenin signaling pathway. Ther Clin Risk Manag 11: 1371-1381, 2015.
38. Ji XK, Xie YK, Zhong JQ, Xu QG, Zeng QQ, Wang Y, Zhang QY and Shan YF: GSK-3β suppresses the proliferation of rat hepatic oval cells through modulating Wnt/β-catenin signaling pathway. Acta Pharmacol Sin 36: 334-342, 2015.
39. Bergmann C, Akhmetshina A, Dees C, Palumbo K, Zerr P, Beyer C, Zwerina J, Distler O, Schett G and Distler JH: Inhibition of glycogen synthase kinase 3β induces dermal fibrosis by activation of the canonical Wnt pathway. Ann Rheum Dis 70: 2191-2198, 2011.
40. Chattopadhyay M, Nath N, Kodela R, Sobocki T, Metkar S, Gan ZY and Kashfi K: Hydrogen sulfide-releasing aspirin inhibits the growth of leukemic Jurkat cells and modulates β-catenin expression. Leuk Res 37: 1302-1308, 2013.
41. Liu C, Xu X, Gao J, Zhang T and Yang Z: Hydrogen sulfide prevents synaptic plasticity from VD-induced damage via Akt/GSK-3β pathway and notch signaling pathway in rats. Mol Neurobiol 53: 4159-4172, 2016.
42. Qu Y, Zhang L, Kang Z, Jiang W and Lv C: Ponatinib ameliorates pulmonary fibrosis by suppressing TGF-β1/Smad3 pathway. Pulm Pharmacol Ther 34: 1-7, 2015.
43. Jin Z, Gu C, Tian F, Jia Z and Yang J: NDRG2 knockdown promotes fibrosis in renal tubular epithelial cells through TGF-β1/Smad3 pathway. Cell Tissue Res 369: 603-610, 2017.
44. Hasan IH, El-Desouky MA, Hozayen WG and Abd el Aziz GM: Protective effect of zingiber officinale against CCl4-induced liver fibrosis is mediated through downregulating the TGF-β1/Smad3 and NF-kB/IkB pathways. Pharmacology 97: 1-9, 2016.
45. Wang XT, Gong Y, Zhou B, Yang JJ, Cheng Y, Zhao JG and Qi MY: Ursolic acid ameliorates oxidative stress, inflammation and fibrosis in diabetic cardiomyopathy rats. Biomed Pharmacother 97: 1461-1467, 2018.
46. Westermann D, Rutschow S, Jager S, Linderer A, Anker S, Riad A, Unger T, Schultheiss HP, Pauschinger M and Tschöpe C: Contributions of inflammation and cardiac matrix metalloproteinase activity to cardiac failure in diabetic cardiomyopathy: The role of angiotensin type 1 receptor antagonism. Diabetes 56: 641-646, 2007.
47. Dong B, Yu QT, Dai HY, Gao YY, Zhou ZL, Zhang L, Jiang H, Gao F, Li SY, Zhang YH, *et al*: Angiotensin-converting enzyme-2 overexpression improves left ventricular remodeling and function in a rat model of diabetic cardiomyopathy. J Am Coll Cardiol 59: 739-747, 2012.
48. Xiao T, Zeng O, Luo J, Wu Z, Li F and Yang J: Effects of hydrogen sulfide on myocardial fibrosis in diabetic rats: Changes in matrix metalloproteinases parameters. Biomed Mater Eng 26 (Suppl 1): S2033-S2039, 2015.
49. Li CJ, Lv L, Li H and Yu DM: Cardiac fibrosis and dysfunction in experimental diabetic cardiomyopathy are ameliorated by alpha-lipoic acid. Cardiovasc Diabetol 11: 73, 2012.
50. Guo Y, Gupte M, Umbarkar P, Singh AP, Sui JY, Force T and Lal H: Entanglement of GSK-3β, β-catenin and TGF-β1 signaling network to regulate myocardial fibrosis. J Mol Cell Cardiol 110: 109-120, 2017.
51. Guo X, Ramirez A, Waddell DS, Li Z, Liu X and Wang XF: Axin and GSK3-control Smad3 protein stability and modulate TGF-signaling. Genes Dev 22: 106-120, 2008.